HTML ABSTRACT + LINKS

Nanoporous Au: A high yield strength material

Juergen Biener,[a] Andrea M. Hodge, Alex V. Hamza, Luke M. Hsiung, and Joe H. Satcher, Jr.
Nanoscale Synthesis and Characterization Laboratory, Lawrence Livermore National Laboratory, P.O. Box 808, L-370, Livermore, California 94550

(Received 14 June 2004; accepted 19 October 2004; published online 23 December 2004)

The plastic deformation of nanoporous Au under compressive stress was studied by depth-sensing nanoindentation combined with scanning electron microscope characterization. The nanoporous Au investigated in the current study exhibits a relative density of 42%, and a spongelike morphology of interconnecting ligaments on a length scale of ~100 nm. The material is polycrystalline with a grain size on the order of 10–60 nm. Microstructural characterization of residual indentation impressions reveals a localized densification via ductile (plastic) deformation under compressive stress and demonstrates the ductile behavior of Au ligaments. A mean hardness of 145(±11) MPa and a Young's modulus of 11.1(±0.9) GPa was obtained from the analysis of the load-displacement curves. The hardness of investigated *np*-Au is ~10 times higher than the hardness predicted by scaling laws of open-cell foams thus potentially opening a door to a class of high yield strength—low-density materials. © *2005 American Institute of Physics*. [DOI: 10.1063/1.1832742]

INTRODUCTION

The formation of nanoporous metallic structures has been primarily studied in the context of alloy corrosion and has been linked to material failure via brittle crack emission.[1–3] More recently, nanoporous metals synthesized by electrochemically driven dealloying of binary alloys have attracted considerable interest due to the potential sensor and actuator applications.[4,5] In general, these materials exhibit an open spongelike structure of interconnecting ligaments with a typical pore size distribution on the nanometer length scale. Despite the progress made in understanding the process of porosity formation during dealloying,[5–8] very little is known about the mechanical properties of nanoporous metals. For example, Li and Sieradzki.[9] reported a ductile-brittle transition in porous Au, which seemed to be controlled by the microstructural length scale of the material. However, the question still remains whether the brittle nature of nanoporous Au is caused by an intrinsic brittleness of Au ligaments on the nanometer length scale or is a consequence of the macroscopic structure.

The discussion above demonstrates that a detailed understanding of the deformation mechanism of nanoporous metals is highly desirable. The mechanical properties of foam materials are generally described in terms of scaling laws. However, it is not clear if these models can be applied to porous materials on the nanometer length scale. In the present work, we investigate the mechanical properties of nanoporous Au with a relative density of 42% employing depth-sensing nanoindentation combined with postindentation microstructural characterization. We observed local densification via ductile, plastic deformation under compressive stress, in contrast to the macroscopic brittleness of the material. The mechanical properties of nanoporous Au, such as yield strength and elastic modulus, are discussed in the context of scaling laws.

EXPERIMENT

The nanoporous Au samples used in the present study were made by electrochemically driven dealloying. A polycrystalline $Au_{0.42}Ag_{0.58}$ alloy ingot was prepared by arc-melting Au (99.999%) and Ag (99.999%). The sample was homogenized by annealing for ~100 h at 900 °C. Approximately 0.5-mm-thick disks were cut from the alloy ingot, heat treated for 8 h at 800 °C, and polished on one side. The alloy composition was confirmed by a fire assay technique.

Nanoporous Au samples were prepared by selective electrolytic dissolution of Ag from the $Au_{0.42}Ag_{0.58}$ alloy.[10] A three-electrode electrochemical cell controlled by a potentiostat (Princeton Applied Research, Model 363) was used for these experiments. Dealloying was performed at room temperature, using a platinum wire as a counter electrode and 75% nitric acid as an electrolyte. The alloy samples were held at an applied electrochemical potential of ~1 V (versus a saturated calomel electrode) for a period of 2–3 days until no further weight loss was detected. Energy dispersive x-ray (EDX) spectra collected from the nanoporous Au samples confirm that Ag was almost completely removed during dealloying.

Scanning electron microscopy (SEM), transmission electron microscopy (TEM), and x-ray diffraction (XRD) were employed for microstructural characterization. TEM samples were prepared by microtome slicing. The mechanical properties of nanoporous Au were tested by depth-sensing nanoindentation using a Triboindenter (Hysitron). Both Berkovich (tip radius of ~200 nm) and conospherical (tip radius of ~1 μm) indenter tips were used for the current experiments. Indentations were performed on the planar, "polished surface" (polished before dealloying) of the

[a]Author to whom correspondence should be addressed; electronic mail: biener2@llnl.gov

 © 2005 American Institute of Physics

Downloaded 15 Sep 2006 to 128.115.27.10. Redistribution subject to AIP license or copyright, see http://jap.aip.org/jap/copyright.jsp

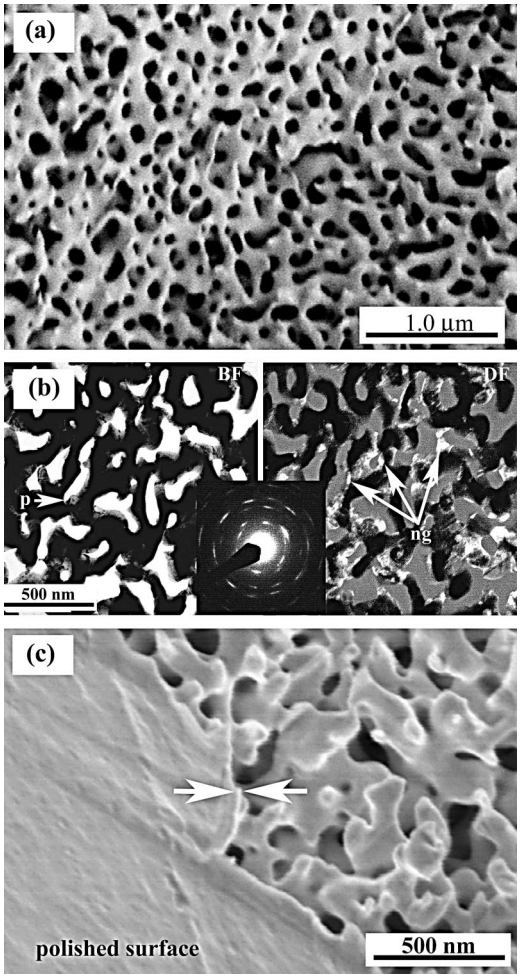

FIG. 1. Microstructure of nanoporous Au: (a) SEM micrograph showing the characteristic spongelike structure of nanoporous Au bulk material. The typical length scale of both ligaments and pores is in the order of ~100 nm. (b) Bright-field (left) and dark-field (right) TEM images demonstrating the morphology of nanoporous Au as well as the grain structure of the Au ligaments. Pores (*p*) and nanograins (ng) are indicated by arrows. The selected area diffraction pattern shown in the inset proves the polycrystalline character of the nanoporous Au sample (c) SEM micrograph of the "polished" surface. The nanoporous structure of the bulk sample is terminated by an ~10–20-nm-thick film of dense Au (indicated by arrows).

sample disks as well as on the cross sections produced by fracturing the sample. The latter exhibits a very rough surface morphology, but allows visualizing the deformation mechanism by post indentation microstructural characterization. All nanoindentation experiments were performed using a constant loading rate of 250 μN/s with loads ranging from 200 to 1800 μN.

RESULTS AND DISCUSSION

Dealloying of $Au_{0.42}Ag_{0.58}$ yields an open spongelike structure of interconnecting ligaments with a unimodal pore size distribution, in agreement with the literature.[5–7,11] SEM images collected from a fractured sample reveal the morphology of nanoporous Au [Fig. 1(a)]. Both ligament width and pore size are homogenous throughout the bulk of the material, and the typical length scale is 100 nm. XRD reveals that the material is polycrystalline with a face-centered-cubic (fcc) structure, and a line broadening analysis suggests

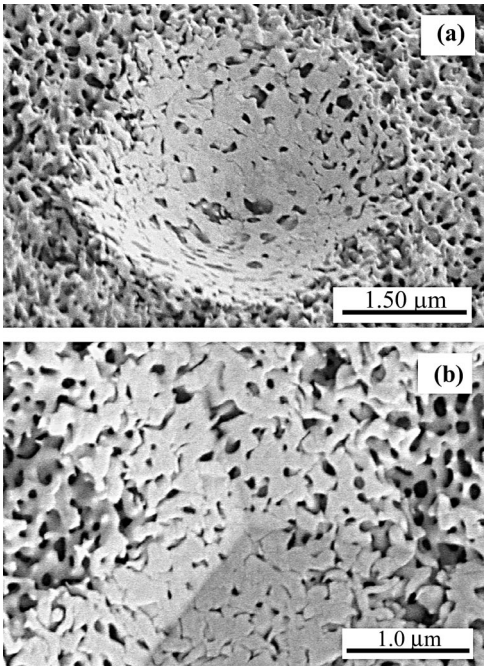

FIG. 2. SEM micrographs of 8000-μN indentations on a fractured surface of nanoporous gold: (a) conospherical tip with a tip radius of ~1 μm, and (b) Berkovich tip with a curvature of ~200 nm. Ductile densification is observed for both probes. Note that the plastic deformation is confined to the area under the indenter, and adjacent areas are virtually undisturbed.

a crystallite size of 30 nm. TEM images confirm the polycrystalline character of our nanoporous gold sample with a broad grain-size distribution between 10 and 60 nm [Fig. 1(b)]. The good agreement between the XRD and TEM results suggests that the line broadening analysis is not affected by residual stress. The bulk structure is terminated by a very thin 10-20 nm thick surface layer of pure Au, which seems to be free of pores, at least in the resolution limit of our SEM [Fig. 1(c)]. The nanoporous structure starts abruptly under this dense surface layer without any further transition region. Thus the presence of the thin layer of compact material on top of the nanoporous material should not give rise to complications during depth-sensing nanoindentation.

The dominant deformation mechanism during nanoindentation in nanoporous Au is ductile, plastic densification. Figure 2 shows SEM micrographs of 8000-μN peak load indentations on the fracture surface using a conospherical (a) and a Berkovich tip (b), respectively. A close inspection of the residual impressions reveals that the deformation is confined in the contact area and dominated by a ductile densification. Note that the pore structure adjacent to the indents is undisturbed. This clearly demonstrates the absence of strong long-range stress fields. Brittle fracture or crack emission was *not* observed, even for a sharp wedge indenter such as the Berkovich tip. The ductile deformation under compressive stress observed here is in contrast to the brittle nature of nanoporous Au under tensile stress reported in the literature.[2,3,9]

The ductile deformation of nanoporous Au under compressive stress is further demonstrated by the load-displacement (*P*-*h*) indentation curves displayed in Fig. 3. These experiments were performed on the "polished" surface

Downloaded 15 Sep 2006 to 128.115.27.10. Redistribution subject to AIP license or copyright, see http://jap.aip.org/jap/copyright.jsp

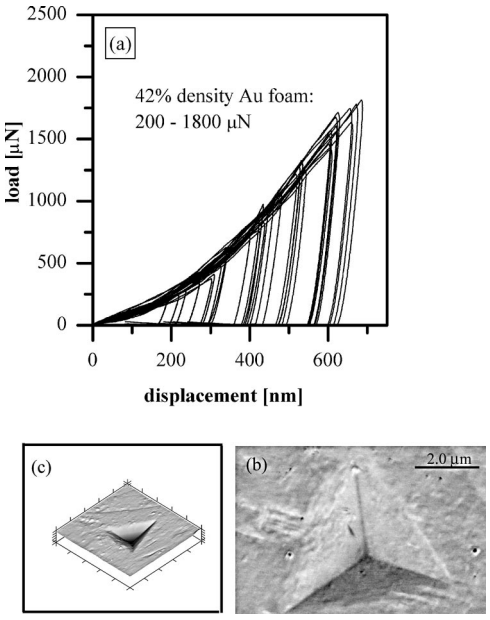

FIG. 3. Top: Series of load vs displacement (P-h) curves collected on the "polished" surface of nanoporous Au using a Berkovich tip. The peak load was adjusted from 200 to 1800 μN while keeping the loading rate constant at a value of 250 μN/s. Bottom: (a) SPM image (15 μm$\times$15 μm) obtained by using the imaging capabilities of the Hysitron TriboIndenter, and (b) SEM images of a Berkovich indent made with a peak load of 1815 μN.

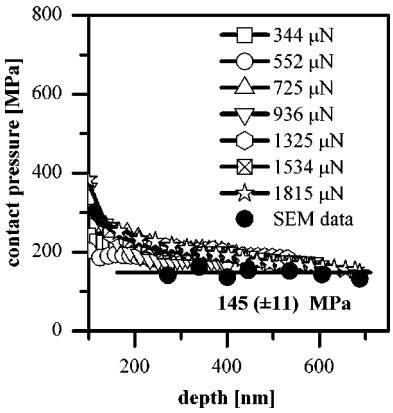

FIG. 4. Contact pressure vs depth curves calculated from the load-depth curves shown in Fig. 3. The contact pressure p_c can be directly obtained from the relationship $p_c = P/A(h)$, where P is the applied load, and A is the projected contact area between the sample and the indenter as a function of the total indentation depth h.

of the sample to minimize the effect of surface roughness. The peak load ($P_{\max}$) was increased from 200 to 1800 μN, resulting in maximum indentation depths between 180 and 700 nm. The experiment does not test the mechanical properties of individual ligaments but senses the mechanical response of a large number of ligaments and pores as the typical ligament width is in the order of 100 nm, and the Berkovich tip used for this particular experiment had a curvature radius of ~200 nm. Considering the inherent inhomogeneity of a random porous material, the reproducibility of the experiment as judged by the overlapping loading sections of the P-h curves is surprisingly good, and the influence of surface roughness on the curves seems to be negligible. Similar data sets were obtained from many different sample positions.

The residual indent impressions on the "polished" surface were studied by scanning probe microscopy (SPM) and SEM to further analyze the deformation mechanism of nanoporous Au. Both SPM [Fig. 3(b)] and SEM [Fig. 3(c)] images of the indents reveal that the deformation is contained in the contact area. Neither pileup of material nor deformation adjacent to the residual impression was observed. These observations are consistent with the experiments performed on the fracture surface (Fig. 2) and indicate a local densification underneath the indenter tip, i.e., a nonvolume conserving ductile deformation mechanism.

A mean contact pressure of 180 MPa was determined from load-depth curves (Fig. 3) by replotting the data as pressure-depth curves shown in Fig. 4. The contact pressure p_c, which is equivalent to the hardness value H, can be directly obtained from the relationship $p_c = P/A(h_c)$, where P is the applied load, and A is the projected contact area as a function of the contact depth h_c calculated from the calibrated tip area function. As recently pointed out by Toivola *et al.*,[12] densifying materials such as the nanoporous Au studied here do not show elastic deformation adjacent to the indent, and the contact depth h_c can be replaced by the total indentation depth h. The resulting contact pressure-depth curves are displayed in Fig. 4. Only data points for indentation depths in excess of 100 nm were considered to minimize the effect of surface roughness. The pressure-depth plot shown in Fig. 4 reveals an almost constant contact pressure of ~180 MPa for indentation depths in excess of ~200 nm, i.e., work hardening is not observed, at least not in the investigated depth range. The increasing hardness with decreasing indentation depth below 200 nm can be attributed to an indentation size effect[13] and is consistent with the observations reported by Corcoran *et al.*[14]

Hardness values were also calculated from the ratio of the peak indentation load $P_{\max}$ to the projected indentation area A_p of the residual impression. The projected indentation area was obtained from postindentation SEM images of the residual impressions [Fig. 3(c)]. The mean hardness obtained by this procedure is 145 (±11) MPa, very similar to the contact pressure obtained from the contact pressure-depth data shown in Fig. 4. This further proves that the deformation during indentation is predominately plastic, and only very little elastic recovery is observed during the unloading section of the experiment.

The yield strength σ of nanoporous Au was assessed from the hardness values obtained by the indentation experiments described above. In the case of dense metals, the yield strength σ_s is related to the hardness H by $\sigma_s = \frac{1}{3}H$. However, in the case of porous metals, deformation under the indenter is not constrained by the surrounding material due to densification. Thus the indentation test acts like a uniaxial compression test, and the yield strength σ is simply equal to the hardness, $\sigma = H$.[13,15] According to this relationship, the yield strength σ of nanoporous Au investigated in the present study is ~145 MPa.

The yield strength can be compared to the value predicted by scaling laws. Treating nanoporous Au as an open-

Downloaded 15 Sep 2006 to 128.115.27.10. Redistribution subject to AIP license or copyright, see http://jap.aip.org/jap/copyright.jsp

TABLE I. Summary of the mechanical properties of nanoporous Au with a relative density of 42%. The values predicted by scaling laws were obtained by using the indicated reference values for the solid material.

Nanoporous Au 42% density	Experiment	Scaling law	Reference value
Yield strength σ (MPa)	145 (±11)	16	200[a]
		122–653	1500–8000[b]
Young's Modulus E (GPa)	11.1 (±0.9)	10.1–15.0	57–85[c]

[a]Macroscopic yield strength of Au, Ref. 17.
[b]Intrinsic yield strength of Au, Refs. 18–21.
[c]Literature value of the Young's modulus of Au, Refs. 20 and 24.

cell foam, the yield strength σ of nanoporous Au should be related to the relative density (ρ_{np}/ρ_s) by Eq. (1),

$$\sigma = C_1\sigma_s(\rho_{np}/\rho_s)^n, \tag{1}$$

where σ_s and ρ_s are the yield strength and the density of the solid material, and ρ_{np} is the density of nanoporous Au.[15] The proportionality constant C_1 describes the cell geometry and the density exponent n depends on the deformation mechanism of the cell. Experimental data indicate that a wide range of open-cell foam materials can be adequately described by $C_1=0.3$ and $n=3/2$.[15,16] Using the literature value[17] for the macroscopic yield strength of Au, $\sigma_s=200$ MPa, Eq. (1) predicts that the yield strength of nanoporous Au with 42% relative density is ~16 MPa. Thus the experimentally determined value of the yield strength is ~10 times larger than the value predicted by scaling laws, i.e., 145 MPa instead of 16 MPa. This discrepancy gives rise to the question if the scaling laws deduced from macroscopic foams can be applied to nanoporous materials. However, if we assume that Eq. (1) correctly describes the mechanical properties of nanoporous Au, the experimentally determined value of 145 MPa for the yield strength of nanoporous Au would require that the yield strength of the solid material σ_s is in the order of ~1.8 GPa. This interpretation suggests that the yield strength of the ligaments in nanoporous Au approaches the intrinsic yield strength of gold which is in the order of 1.5–8 GPa.[18–21] The yield strength data of nanoporous Au are summarized in Table I.

The elastic modulus of nanoporous Au was extracted from the unloading curves using standard deconvolution techniques.[22] The analysis reveals a Young's modulus of 11.1 (±0.9) GPa (assuming a Poisson's ratio near zero),[23] independent of contact depth. The constant value of the Young's modulus as a function of indentation depth suggests that the influence of the compact Au surface layer is negligible. Treating nanoporous Au as an open-cell foam, the Young's modulus E can be described by Eq. (2),

$$E = C_2E_s(\rho_{np}/\rho_s)^n, \tag{2}$$

where E_s is the Young's modulus of solid Au, and ρ_{np}/ρ_s is the relative density of the foam.[15] In analogy to Eq. (1), the proportionality constant C_2 describes the cell geometry and the density exponent n describes the elastic cell deformation via ligament bending. Experimental data obtained from open-cell foam materials are usually well fitted by using $C_2=1$ and $n=2$.[15] Assuming that our nanoporous Au sample exhibits a relative density of 42% and using the Young's modulus of Au single crystals as a reference, $E_s=57-85$ GPa,[20] the scaling law would predict a Young's modulus of 10.1–15.0 GPa. Thus the Young's modulus predicted by the scaling law is in the same magnitude of order than the experimentally observed Young's modulus of 11.1 (±0.9) GPa.

CONCLUSIONS

The experiments described in this article clearly demonstrate the ductile, plastic behavior of nanoporous Au under compressive stress. Localized densification under the indenter tip indicates the absence of strong long-range stress fields. Brittle fracture or crack emission was not observed. This clearly evidences the intrinsic ductile behavior of Au ligaments in nanoporous Au. The experimentally determined Young's modulus of ~11 GPa is in the same magnitude of order than the value predicted by scaling laws, and the hardness of ~145 MPa suggests that the yield strength of the ligaments in nanoporous Au approaches the intrinsic yield strength of gold.

ACKNOWLEDGMENTS

This work was performed under the auspices of the U.S. Department of Energy by University of California, Lawrence Livermore National Laboratory under Contract No. W-7405-Eng-48. The authors would like to thank A. Bliss for sample preparation and J. Ferreira for SEM characterization.

[1]K. Sieradzki and R. C. Newman, Philos. Mag. A **51**, 95 (1985).
[2]F. Friedersdorf and K. Sieradzki, Corros. Sci. **52**, 331 (1996).
[3]R. G. Kelly, A. J. Frost, T. Shahrabi, and R. C. Newman, Metall. Trans. A **22**, 531 (1991).
[4]J. Weissmuller, R. N. Viswanath, D. Kramer, P. Zimmer, R. Wurschum, and H. Gleiter, Science **300**, 312 (2003).
[5]J. Erlebacher, M. J. Aziz, A. Karma, N. Dimitrov, and K. Sieradzki, Nature (London) **410**, 450 (2001).
[6]R. C. Newman, S. G. Corcoran, J. Erlebacher, M. J. Aziz, and K. Sieradzki, MRS Bull. **24**, 24 (1999).
[7]J. Erlebacher and K. Sieradzki, Scr. Mater. **49**, 991 (2003).
[8]K. Sieradzki, R. R. Corderman, K. Shukla, and R. C. Newman, Philos. Mag. A **59**, 713 (1989).
[9]R. Li and K. Sieradzki, Phys. Rev. Lett. **68**, 1168 (1992).
[10]K. Sieradzki, N. Dimitrov, D. Movrin, C. McCall, N. Vasiljevic, and J. Erlebacher, J. Electrochem. Soc. **149**, B370 (2002).
[11]Y. Ding and J. Erlebacher, J. Am. Chem. Soc. **125**, 7772 (2003).
[12]Y. Toivola, A. Stein, and R. F. Cook, J. Mater. Res. **19**, 260 (2004).
[13]A. C. Fischer-Cripps, *Nanoindentation* (Springer, New York, 2002).
[14]S. G. Corcoran, R. J. Colton, E. T. Lilleodden, and W. W. Gerberich, Phys. Rev. B **55**, 16057 (1997).
[15]L. J. Gibson and M. F. Ashby, *Cellular Solids: Structure and Properties*, 2nd ed. (Cambridge University Press, Cambridge, 1997).
[16]R. Brezny and D. J. Green, Annu. Rev. Mater. Sci. **38**, 2517 (1990).
[17]U. Landman, W. D. Luedtke, and J. P. Gao, Langmuir **12**, 4514 (1996).
[18]N. Agrait, G. Rubio, and S. Vieira, Phys. Rev. Lett. **74**, 3995 (1995).
[19]A. Stalder and U. Durig, Appl. Phys. Lett. **68**, 637 (1996).
[20]J. D. Kiely and J. E. Houston, Phys. Rev. B **57**, 12588 (1998).
[21]A. Stalder and U. Durig, J. Vac. Sci. Technol. B **14**, 1259 (1996).
[22]W. C. Oliver and G. M. Pharr, J. Mater. Res. **7**, 1564 (1992).
[23]O. B. Olurin, N. A. Fleck, and M. F. Ashby, Scr. Mater. **43**, 983 (2000).
[24]*Metals Handbook*, 2nd ed. (American Society for Metals ASM International, Metals Materials Park, OH, 1998).

Downloaded 15 Sep 2006 to 128.115.27.10. Redistribution subject to AIP license or copyright, see http://jap.aip.org/jap/copyright.jsp